RESPONSE TO THE REVIEWS

Response to referee 1.

Answers to the major comments

1. The novelties of version 6.0 and the differences between this paper and Vries and Döös (2001) is now stated in the two first paragraphs in the introduction.

2. The reason for now citing and discussing the differences with Chu and Fan (2014) is that we simply do not agree with their approach and their results. This would require a separate study, which would be beyond the scope of this paper. In their experiment they fail to keep the trajectories along the stream lines for the Stommel Gyre, which TRACMASS is able to do with all its schemes. We have discussed together with Bruno Blanke to submit a note on this issue with the Chu and Fan (2014) paper.

Minor comments

- page 1, line 24: perhaps good to define what"s meant with a "grid cell" here. A model grid cell?

Answer: We have added the word "model"

- page 2, line 14: What type of "continuous interpolation" is meant? Spline? Linear?

Answer: We have added the word "linear".

- page 3, line 23: This discussion of mass and volume interchangeability in OGCMs of course is only true in hydrostatic models (also page 4, line 17).

Answer: We have rewritten this now making it clear it is only valid for models that are incompressible.

- page 6, line 20: This comment about how TRACMASS works on any vertical grid has been made already, and there is probably no need to mention it again here

Answer: We have removed this paragraph.

- page 8, line 6: Are there any physical interpretations for α, β, γ and δ? In particular for α, what kind of flow is $\alpha > 0$ versus $\alpha < 0$

Answer: We have added a physical interpretations for α at the end of section 2.4.1 and 2.4.2

- page 10, line 14: The terminology of grid cell boundaries is a bit confusing at times. Here it is called a "wall", even though it is not a land-sea boundary. I suggest to carefully go through the manuscript to standardise the wording used to distinguish ocean-ocean (or atmosphere-atmosphere) grid faces from land-ocean faces.

Answer: We have replace the words "wall" and "grid-box wall" by "grid face" in the entire text.

- page 10, line 27: Would be good to explicitly mention which root-solving algorithm is used.

Answer: Done.

- page 11, line 28: "Conveyor Belt" is a simplistic term here, better to call it thermohaline circulation?

Answer: We do not agree with this. Any circulation in T-S space can be defined as thermohaline but the Agulhas rings flowing north into the Atlantic are part of a global circulation often referred to as the "Conveyor Belt".

- page 11, line 29: How are the particles seeded in the vertical? At all depth levels?

Answer: Yes, at all depths, which we have added in the text now.

- page 12: There appears to be no reference to Figure 5 in the text between the first references to Figure 4 and Figure 6?

Answer: Fig. 5 is now references to between Fig. 4 and Fig. 5.

- page 16: refer to Lacasce (2008) here, for the standard work on the statistics of particle dispersion in the ocean?

Answer: We are now citing Lacasce (2008) in this appendix.

- Figure 4: What does the colouring of the trajectories represent? And it might also be useful to add a grid with selected longitudes and latitudes, so that reader unfamiliar with the Agulhas region can orient themselves (that latter point also for Figure 9)

Answer: We have added "Colouring used to separate the trajectories from each other.

- Figure 7: Beyond showing the mean distance, would it also be useful to show the spread (e.g. the one standard deviation of each line with time)?

Answer: That is basically what the relative dispersion shows

- Figure 8: The presentation of Fig 8 is not ideal, because most lines fall on top of each other. I appreciate that this is the whole point of the Figure, but a quick reader might be confused where the other lines are. Is there no better way to show that 6 of the 7 lines essentially lay on top of each other?

Answer: We have tried different solution but the fact that the line lay on top of each other just reflects that they give very similar results.

Type-os etc: - page 2, line 18: Replace "always" with "typically"?

Answer: Done.

- page 2, line 23: "behind these can be found"

Answer: Changed.

- page 5, line 23: should be Eq (19)?

Answer: No.

- page 9, line 16: Eq 32 should not be part of this list?

Answer: Yes and it is written Eqs. (31)-(34), which includes Eq. 32.

- page 9, line 18: There is no following subsection, there is just the text below - page 10, line 10: use "domain" rather than "?box?"?

Answer: True and we have rewritten the text and deleted "following subsection".

- page 10, line 28: "r" at end of line misses subscript i

Answer: Added an index i to this r.

- page 11, line 20: "implies that they"

Answer: Changed as suggested

- page 12, line 16: "distances have been possible to compute since all"

Answer: The extra "been" has been removed.

Response to referee Griffies

General comments

1. As detailed here, and in the earlier literature, the TRACMASS approach performs an analytic integration of the trajectory within a grid cell. This point is emphasized in the present manuscript. Importantly, this integration is enabled by an **assumption** that the subgrid scale velocity components are linear functions of their corresponding directions: [u(x), v(y), w(z)]. Surprisingly, this critical assumption is not explicity noted in the present manuscript. It should in fact be emphasized and defended.

How/where will it break down? As written, words such as "the trajectory solutions are exact" (pg 5, line 10) make it look like TRACMASS is performing magic. Instead, it is following an exact treatment based on the assumption of subgrid [u(x), v(y), w(z)].

Answer: We have added a few sentences on this in the first paragraph of section 2 and section 2.2 to better highlight this key assumption. We agree that the use of the word "exact" may mislead readers, and have rewritten a few sentences such as p5, line10 to emphasise that the trajectories are solutions to a differential equation, and that there is nothing magical about it.

2. The differential equations for the position within a grid cell are given by equation (17) for the stationary case, and equation (26) for the time-dependent case. Both equations are offered to the reader as if they should be an obvious consequence of something a priori. However, both equations need more build up to motivate and rationalize. The only statement to suggest where equation (17) comes from is line 19 on pg 5: "The transport and position within the grid box are now related by U = dr/dx...". However, this is a statement that offers no motivation nor a derivation. What is the basis for this relation?

So as written, equations (17) and (26) seemingly appear from no where, and the reader is left scratching his/her head. Sans shared intuition, these equations remain mere black boxes to the reader, which is of no use to the reader.

Answer: We have rewritten the first paragraphs of section 2.2 (stationary scheme) and 2.4 (time-dependent scheme) to better lead up to the differential equations that we use to calculate trajectories. We hope this is clearer to the reader.

3. At the end of Section 2, I found myself wanting to see a clear schematic to summarize the stationary method and the time-dependent method. Likely these schematics appear in the basic literature. But given that you are rederiving the methods here, it would serve the reader well to have such schematics presented again, perhaps in an updated manner. These schematics could offer far more conceptual understanding than the maths presented in Section 2.

Answer: A very good point and we have both added a paragraph at the end of section 2 and a figure, summarising the resulting differences between the schemes within a time-space cell.

4. The word "this" is used many placed without qualifying. The reader is often left wondering what "this" referes to. Please be more careful with letting the reader know what "this" refers to. It is important to do so in order not to lose the reader, especially the novice.

Answer: We have rewritten a number of sentences in order to remove "this".

Minor comments

- page 1, line 24: perhaps good to define what"s meant with a "grid cell" here. A model grid cell?

Answer: Yes and we have now written "model grid cell".

Response to referee 3.

General considerations

1. In section 3 it appears to be taken at face value that the time-dependent case represents a "model truth", to which the other cases are compared. The sentence on P2 L15 suggests that it is "logical" to use a stepwise-stationary scheme that analyses output at the model time-integration frequency. Is there some way of clarifying/demonstrating that the time-dependent solution is the most realistic solution to the model transports? I suppose that a real "truth" could be calculated by outputting the model at every model integration step and then performing the stepwise-stationary analysis. Since this is obviously very laborious, perhaps the authors can provide an easier description.

Answer: We have now included the following sentences in the discussion:"We thus conclude that the "time-dependent" scheme is the most accurate of those tested here for two reasons. Firstly for theoretical reasons since the "time-dependent" scheme does not assume stationary velocities during any period of time. Secondly the trajectories computed with the "stepwise-stationary" scheme converge towards those computed with the "time-dependent" scheme for increasing numer of intermediate time steps. A future study could be to calculate trajectories first using fields stored at each GCM time step and second using fields stored at longer time intervals. In the first case, trajectories would be very accurate and could represent a "truth", and the second case could be used to evaluate which of the two schemes is the closest to the "truth". "

2. P13: L26-29. In order to be able to better interpret those studies that have used the fixed timestep scheme, it would be useful to know if the values provided on e.g. P13 L26-29 are sensitive to the number of particles used and the time period over which the particles are seeded. Is it possible that the fixed GCM time step scheme converges (closer) towards the other schemes when a long(er) seeding period is used along with a large(r) number of particles? In this case, the streamfunctions could be compared to an Eulerian streamfunction that is taken as the actual model truth. Similarly, do the number of particles used in the experiments constitute a "large en- semble".

Answer: We have added at the end of section 3.4: "We have repeated the above ocean-trajectory experiment by releasing the particles in other time periods and increasing the ensemble size. The results only changed marginally."

3) In the absence of having tested a suite of models, I think the authors could be clearer in places (e.g. P15 L20) that their results are specific to the resolutions of their chosen models. While the increased accuracy of the method will certainly translate to a consideration of lower resolution models, the relative importance is likely going to decrease. Perhaps for certain applications the fixed timestep solution could be just as meaningful as the time-dependent one, if a large enough number of particles are integrated?

Answer: "We have here only tested one OGCM and one AGCM simulation, but we speculate that at coarser resolution in both space and time, the differences obtained with the two schemes would increase. However, in non eddying simulations (e.g. 1° ocean models) this may not be true due to the low variability of the flow."

Specific comments

- P1 L3-4. I find a "limited period of time" to be a pretty vague description. Something more like "... stationary for set intervals of time between saved model outputs" might be clearer.

Answer: Done

- P1 L13 At this point in the article, "more accurate" seems ambiguous as to whether it is more accurate w.r.t the time-dependent case or w.r.t itself. Perhaps a change to "increasingly more accurate" would make it clearer.

Answer: Done

- P3 L12: superscript n is not defined until P4. Also, n is sometimes used as a subscript, presumably by mistake (e.g. P3 L24).

Answer: n is now defined where it first used.

- P3 L30: It is not made clear why it is more advantageous or why the direct calculation would be any more accurate than is done by the model. Is it because of the interpolation that is applied by TRACMASS?

Answer: It is because the TRACMASS trajectory schemes rely on mass continuity. Ideally, the two methods should give the same result.

- P4 L7: If Tracmass can work on models in which a variable vertical resolution is also spatially dependent, as stated on P3, then should Δ_z in equation 8 also have subscripts i, j?

Answer: Yes it should. We have added this in all equations where Δz is written.

- P4 L10: Δt_G is defined only later on.

Answer: We have now defined it.

- P4 L14: I'd have thought convention normally has k=0 as the surface grid cell, not the bottom.

Answer: Yes, but in TRACMASS we redefine the index k in order to have increasing index with positive vertical velocity, which makes the code simpler.

- P4 L17: It appears that a numbered list is started here, but I?m not sure why.

Answer:Removed

- equation 13: This has already been written of line 24 of the previous page. Accordingly, could equations 14 and 15 also be moved up to where that previous definition of hydrostatic balance is given, which seems a more natural place for these equations to go? Currently they are returning the discussion to horizontal velocities after having discussed vertical velocities.

Answer: A good point. We have moved equations as suggested.
- P5 L5-9: I feel this section would be more helpful if given at an earlier point in the paper, plus it is largely repeating what was stated on P3 L13.

Answer: We have removed this paragraph and added some text in the beginning of the section instead.

- P5 L16: Perhaps say here that this is done for V and W too.

- P5 L28: Typo Eq (1).

Answer: Done.

Answer: We have rewritten this in order to introduce the meridional and vertical displacements.

- P6 L2. Regarding "if this is not the case", it is not clear whether this is referring to U(r1) or U(r2) being positive, or both.

Answer: We have rewritten this.

- P7 L11-15: It should perhaps say here that both the fixed time step and the stepwise stationary cases will be tested.

Answer: We have added at the end of this section: "These two schemes together with a truly time dependent scheme, described in next section, will be tested."

- Equation 24: typo on the second line of the equation, in the first F term - a subscript n.

Similar typo in equation 38.

Answer: Corrected in both equations.

- Figure 2: What is a "region" here, and why only three of them in subplot (a)? Also, given that the stepwise-stationary method can also include temporal interpolation, it should be stated here that these solutions are for the time-dependent case.

Answer: We now state that this is for the "time-dependent" scheme and we use the word "corner" instead of "region".

- P9 L15: It is not clear whether "this case" is referring to the time-dependent or stepwise case.

Answer: We have rephrased this in order to clarify differences between the two cases.

- P9 L18. The "following subsection" or "this subsection"?

Answer: This sentence has been rephrased.

- Section 3.1: There is no mention of Figure 5.

Answer: We now mention this figure, which is now Fig. 6.

- Figures 5 onwards: Isn't $I_s = 1$ the same as the fixed GCM time step?

Answer: No. $I_S = 1$ *is one average between two GCM outputs.*

- P13 L2: It should perhaps be clarified that this is now referring to improvements in the GCM, not the Lagrangian model.

Answer: This has been clarified and the resolution regards the GCM and the sub-grid parameterisation the Lagrangian model, which was not clear.

- P13 L18: Figure 9 shows neither a subtraction nor the stepwise-stationary case.

Answer: We have this corrected this, which was due to that we had originally other stream functions.

- P13 L20-21: I don't understand this sentence, which appears to contrast with those on lines 26-29 in the same paragraph. C4

Answer: Same correction as for your previous comment.

- P14 L11: Instead of saying "for some time", which is ambiguous, I would suggest something more like "for the duration of a user defined intermediate time step between model output fields". Also, the use of the past tense here doesn't work well, especially since the next sentence is in the present again.

Answer: Thank you for this sentence, which we have now used.

- P14 L13: Similarly, instead of "is in steady state" I would say something more like "is steady during each time step".

Answer: We have changed to "The "time-dependent" scheme does not assume that the velocity is in steady state during any time interval since it solves the differential equations of the trajectory path not only in space but also in time."

Evaluation of oceanic and atmospheric trajectory schemes in the TRACMASS trajectory model v6.0

Kristofer Döös[1], Bror Jönsson[2], and Joakim Kjellsson[3]

[1]Department of Meteorology, Stockholm University, SE-10691 Stockholm, Sweden.
[2]Department of Geosciences, Princeton University, Guyot Hall, Princeton, NJ 08544, USA
[3]Atmospheric, Oceanic, and Planetary Physics, University of Oxford, UK

Correspondence to: Kristofer Döös (doos@misu.su.se)

Abstract. ~~Two~~ Three different trajectory schemes for oceanic and atmospheric general circulation models are compared in two different experiments. The theories of the ~~two~~ trajectory schemes are presented showing the differential equations they solve and why they are mass conserving. One scheme assumes that the velocity fields are stationary for ~~a limited period of time~~ set intervals of time between saved model outputs and solves the trajectory path from a differential equation only as a function of space, i.e. "stepwise stationary". The second scheme ~~uses a~~ is a special case of the "stepwise-stationary" scheme, where velocities are assumed constant between GCM outputs, it uses hence a "fixed GCM time step". The third scheme uses a continuous linear interpolation of the fields in time and solves the trajectory path from a differential equation as a function of both space and time, i.e. "time-dependent". ~~A special case of the "stepwise-stationary" scheme, when velocities are assumed constant between GCM outputs, is also considered, named "fixed GCM time step".~~ The trajectory schemes are tested "off-line", i.e. using the already integrated and stored velocity fields from a GCM. The first comparison of the schemes uses trajectories calculated using the velocity fields from an eddy-resolving ocean general circulation model in the Agulhas region. The second comparison uses trajectories calculated using the wind fields from an atmospheric reanalysis. The study shows that using the "time-dependent" scheme over the "stepwise-stationary" scheme greatly improves accuracy with only a small increase in computational time. It is also found that with decreasing time steps the "stepwise-stationary" scheme becomes increasingly more accurate but at increased computational cost. The "time-dependent" scheme is therefore preferred over the "stepwise-stationary" scheme. However, when averaging over large ensembles of trajectories the two schemes are comparable, as intrinsic variability dominates over numerical errors. The "fixed GCM time step" scheme is found to be less accurate than the "stepwise-stationary" scheme, even when considering averages over large ensembles.

1 Introduction

The Lagrangian view of the ocean and atmospheric circulation describes fluid pathways and the connectivity of different regions, which are not readily obtained from an Eulerian perspective. Lagrangian studies often require trajectory calculations using some algorithm that transforms the Eulerian velocity fields, e.g. winds or currents, into trajectories. Although observed velocities can be used, it is much more common to use velocities simulated by a General Circulation Model (GCM). The purpose of this work is to test the different schemes used in the TRACMASS trajectory model (version 6.0) here named the "fixed GCM time step" (**??**), "stepwise stationary" (**?**) and "time-dependent" (**?**). These schemes have previously only been tested using highly idealised velocity fields. Here we will test them velocity fields simulated by comprehensive GCMs for both the ocean and atmosphere.

The TRACMASS trajectory model (**?**) has been continuously updated through the years since it was first introduced by **?**. Version 6.0 represents the latest version, which includes the ability to run TRACMASS with the "time-dependent" scheme by **?** on GCM fields. TRACMASS now also supports many different types of vertical coordinates used in atmosphere and ocean GCMs. The code has also been made more structured and user friendly.

Their original feature of TRACMASS and the related Ariane model (**?**) is that they solve the trajectory path through each model grid cell with an analytical solution of a differential equation, which depends on the velocities on the ~~walls of the~~ faces of the model grid box. This is different from iterative schemes such as the commonly used 4th-order Runge-Kutta (RK4). The TRACMASS schemes have many advantages, e.g. mass conservation within the grid cell in the same way as the GCM itself, as well as fast trajectory computation. Furthermore, as the solution to the differential equation is unique, trajectories can be calculated forward in time and subsequently backward in time to arrive at exactly the original position, which other trajectory methods, e.g. RK4, can not accomplish. This makes it possible to trace the origins of water or air masses as long as stochastic parameterisations (cf. **?**) are not activated.

The first trajectory scheme tested here, "fixed GCM time step", is strictly only valid for stationary velocity fields. It can, however, be used with time-varying velocity fields by dividing the time between GCM outputs into intermediate steps and assuming velocities are stationary during the step. The velocities in an intermediate step are found by linear interpolation between two GCM outputs and hence named "stepwise stationary". However, using intermediate steps increases the computational cost. The "time-dependent" scheme does not assume that the fields are stationary and uses instead continuous bilinear interpolation both in space and time.

The fact that the "stepwise-stationary" scheme uses stepwise-stationary velocities is logical when the scheme is used "on-line", i.e. integrated into a GCM and thus having the same time step as the GCM itself. When the scheme is used "off-line", i.e. separately from the GCM and after the velocity fields have been stored, the time step is the time between two GCM outputs, which ~~always~~ typically is a much longer period than the GCM time step. As the "stepwise-stationary" scheme assumes that velocities are constant during the time step of the trajectory scheme, processes faster than the GCM output frequency are lost.

An alternative to the "stepwise-stationary" scheme was introduced by **?**, where the trajectory solution was not only solved analytically in space as was done by **?**, as well as **?**, but also analytically in time between the GCM outputs. This leads to a more complex differential equation to be solved and integrated as the trajectory progresses through space and time (**?**). The advantage of this "time-dependent" scheme by **?** is that it does not require any intermediate time steps between the model output times and can instead be integrated analytically between the GCM outputs. This in contrast to the "fixed GCM time step" scheme by **?** and the "stepwise stationary" by **?** as well as schemes such as Euler forward or RK4 methods (**??**), where the trajectories are integrated forward in time with as short time steps as possible. A comprehensive review of different trajectory codes as well as the fundamental kinematic framework behind these can be found in **?**.

In section 2 we describe the ~~two~~ three different trajectory schemes and how they are integrated in time in both Ocean General Circulation Models (OGCMs) and Atmospheric General Circulation Models (AGCMs). In section 3 we test the ~~two~~ three trajectory schemes with two different velocity fields, one from an OGCM and one from an AGCM, using various statistics. This study is concluded in section 4 with a summary and discussion of the main results of the trajectory schemes and their tests.

2 Trajectory scheme theory

The trajectory schemes used in TRACMASS are all mass conserving but make different assumptions regarding the time evolution of the Eulerian velocity and pressure fields. The schemes rely on the assumption that, within a grid cell the three velocities components are only linear functions of their corresponding directions, i.e. $u = u(x)$, $v = v(y)$ and $w = w(z)$. An alternative approach is to assume that $u = u(x,y,z)$, $v = v(x,y,z)$ and $w = w(x,y,z)$, which might be more accurate in terms of subgrid velocity but would break mass conservation, since it does not satisfy the discretised continuity equation in a GCM. The trajectory schemes integrate the trajectories from the volume or mass transports through the grid-box ~~walls~~ faces in contrast to many other trajectory schemes that only use the velocity fields. We will first describe how these fluxes are computed and then the ~~two~~ three different trajectory schemes.

2.1 Mass and volume flux

The TRACMASS trajectory schemes are mass conserving as they, like the GCM, deal with the transport across the grid ~~walls~~ faces and the transport is only interpolated linearly between the two opposite ~~walls~~ faces in a grid box. The trajectories will hence never cross a grid boundary.

A GCM mesh is generally spherical or curvilinear. The longitudinal ($\Delta x_{i,j}$) and the latitudinal ($\Delta y_{i,j}$) grid lengths will hence be functions of their horizontal positions i,j on a curvilinear grid. The vertical coordinate in an GCM has a depth level thickness $\Delta z^n_{i,j,k}$, where k is vertical level, and n is time step. Note that the vertical resolution can vary not only vertically but also both horizontally and in time, which makes it possible to use any vertical coordinate ~~such as~~ e.g. sigma (?), z-star, pressure or hybrid coordinates (?). The horizontal mass transports through the eastern and northern ~~walls~~faces, respectively, of the i,j,k grid box at time step n are given by

$$U^n_{i,j,k} = \rho^n_{i,j,k} u^n_{i,j,k} \Delta y_{i,j} \Delta z^n_{i,j,k}, \tag{1}$$

$$V^n_{i,j,k} = \rho^n_{i,j,k} v^n_{i,j,k} \Delta x_{i,j} \Delta z^n_{i,j,k}. \tag{2}$$

The zonal velocity $u^n_{i,j,k}$ and the meridional velocity $v^n_{i,j,k}$ are in the above equations on a C-grid. It is, however, possible to use the velocities from A and B-grid models, where the velocities are instead at the corners of the grid cell, leading to

$$U^n_{i,j,k} = \rho^n_{i,j,k} \tfrac{1}{2} \left(u^n_{i,j,k} + u^n_{i,j-1,k} \right) \Delta y_{i,j} \Delta z^n_{i,j,k}, \tag{3}$$

$$V^n_{i,j,k} = \rho^n_{i,j,k} \tfrac{1}{2} \left(v^n_{i,j,k} + v^n_{i-1,j,k} \right) \Delta x_{i,j} \Delta z^n_{i,j,k}. \tag{4}$$

This averaging of two horizontal grid points in order to have the perpendicular velocity to the grid box in the middle on the grid ~~wall~~ face is exactly how a B-grid model discretises the equations, when e.g. solving the continuity equation.

Note that ~~due to incompressibility in the ocean, the~~ the mass transport can be replaced by the volume transport in ~~OGCMs but not in AGCMs. However, in AGCMs~~models that assumes the fluid to be incompressible, which is the case for most OGCMs. In other models (most AGCMs), we may use the hydrostatic approximation to write $\cancel{\rho_{i,j,k,n}\Delta z_{i,j,k,n} = g^{-1}\Delta p_{i,j,k,n}}$

$$\Delta p^n_{i,j,k} = \rho^n_{i,j,k}\, g\, \Delta z^n_{i,j,k}\,. \tag{5}$$

where g is gravity and p is air pressure. The mass transports through the lateral grid faces in the AGCM expressed by Eqs. (1, 2) will use Eq. (5) to determine Δz and hence become

$$U^n_{i,j,k} = u^n_{i,j,k}\Delta y_{i,j}\Delta p^n_{i,j,k}/g \tag{6}$$

$$V^n_{i,j,k} = v^n_{i,j,k}\Delta x_{i,j}\Delta p^n_{i,j,k}/g. \tag{7}$$

The vertical mass transport can similarly be computed from the vertical velocity $w_{i,j,k}$ through the upper ~~wall~~ face of the grid box so that

$$W^n_{i,j,k} = \rho_{i,j,k} w^n_{i,j,k}\Delta x_{i,j}\Delta y_{i,j}\,. \tag{8}$$

The vertical velocity would in the equation above be taken directly from the stored velocity fields from the GCM. It is, however, ~~advantageous~~ in order to guarantee mass conservation, advantageous to instead calculate the vertical transport $W^n_{i,j,k}$ from the continuity equation as the TRACMASS trajectory schemes rely on mass or volume continuity.

The continuity equation, which expresses conservation of mass, states that

$$\frac{\partial \rho}{\partial t} + \frac{\partial(\rho u)}{\partial x} + \frac{\partial(\rho v)}{\partial y} + \frac{\partial(\rho w)}{\partial z} = 0\,. \tag{9}$$

Integrating Eq. (9) over a finite grid box of volume $\Delta x \Delta y \Delta z$ we obtain

$$\frac{\partial M_{i,j,k}}{\partial t} + U_{i,j,k} - U_{i-1,j,k} + V_{i,j,k} - V_{i,j-1,k} + W_{i,j,k} - W_{i,j,k-1} = 0\,, \tag{10}$$

where $M_{i,j,k}$ is the mass of the grid box. The rate of mass change of the grid box $\partial M_{i,j,k}/\partial t$ can on the other hand be due to 1) compression in an ~~AGCMs~~ compressible GCM and/or to 2) grid-box volume change, which generally in a GCM is due to the time dependence of the vertical resolution so that the thickness of model layers vary in time.

The mass of the grid box is

$$M^n_{i,j,k} = \rho^n_{i,j,k}\Delta x_{i,j}\Delta y_{i,j}\Delta z_{\cancel{k}\,i,j,k}{}^{n}\,, \tag{11}$$

where n is the time level of the stored GCM fields so that time is $t = n\Delta t_G$ and Δt_G is the time interval between two stored GCM fields.

The vertical mass transport through the top of the grid box is obtained by discretising Eq. (10) between two stored time levels:

$$W^n_{i,j,k} = W^n_{i,j,k-1} - \left[U^n_{i,j,k} - U^n_{i-1,j,k} + V^n_{i,j,k} - V^n_{i,j-1,k} + \frac{(\rho^{n+1}_{i,j,k}\Delta z^{n+1} - \rho^n_{i,j,k}\Delta z^n)}{\Delta t_G} \frac{(\rho^{n+1}_{i,j,k}\Delta z^{n+1}_{i,j,k} - \rho^n_{i,j,k}\Delta z^n_{i,j,k})}{\Delta t_G} \Delta x \Delta y \right], \tag{12}$$

which is computed by integration from the bottom and upwards with the bottom boundary condition $W_{i,j,0} = 0$. This is the same way the vertical velocity is computed in the GCM except that we use the stored horizontal velocities and the grid-size thicknesses to ensure that they satisfy the time dependency correctly.

~~1)~~ In the case of an OGCM, the fluid is incompressible and thus the density is constant and ρ can be dropped from all equations in order to have volume flux instead of mass flux in the calculations. The vertical volume transport through the top of the grid box becomes

$$W^n_{i,j,k} = W^n_{i,j,k-1} - \left[U^n_{i,j,k} - U^n_{i-1,j,k} + V^n_{i,j,k} - V^n_{i,j-1,k} + \frac{(\Delta z^{n+1} - \Delta z^n)}{\Delta t_G} \frac{(\Delta z^{n+1}_{i,j,k} - \Delta z^n_{i,j,k})}{\Delta t_G} \Delta x \Delta y \right]. \tag{13}$$

~~2)~~ If, additionally, the vertical resolution is time independent, the last term can be neglected and thus

$$W^n_{i,j,k} = W^n_{i,j,k-1} - \left(U^n_{i,j,k} - U^n_{i-1,j,k} + V^n_{i,j,k} - V^n_{i,j-1,k} \right). \tag{14}$$

~~3)~~ On the other hand, in many AGCMs there is both compressibility of the air and a time dependence of the vertical resolution, which is generally expressed in pressure and hence

$$W^n_{i,j,k} = W^n_{i,j,k-1} - \left[U^n_{i,j,k} - U^n_{i-1,j,k} + V^n_{i,j,k} - V^n_{i,j-1,k} + \frac{(\Delta p^{n+1}_{i,j,k} - \Delta p^n_{i,j,k})}{g \Delta t_G} \Delta x \Delta y \right], \tag{15}$$

where ~~g is the gravitational acceleration and the pressure difference Δp between the bottom and top of the grid box is obtained using the hydrostatic approximation:~~

$$\Delta p^n_{i,j,k} = \rho^n_{i,j,k}\, g\, \Delta z^n .$$

~~The mass transports through the lateral grid walls in the AGCM expressed by Eqs. (1, 2) will also use Eq. (5) to determine Δz and hence become~~

$$U^n_{i,j,k} = u^n_{i,j,k} \Delta y_{i,j} \Delta p^n_{i,j,k}/g$$

$$V^n_{i,j,k} = v^n_{i,j,k} \Delta x_{i,j} \Delta p^n_{i,j,k}/g.$$

~~TRACMASS can handle the following different sorts of vertical coordinates: 1) depth-level models, 2) sigma-coordinate models, where the thickness depends on the total depth, which varies in each horizontal grid point, 3) z-star coordinates, where the layer thicknesses depend on sea surface elevation, 4) isopycnal models, where Δz is the density layer thickness, an approach that was that was first usedin TRACMASS by ? and 5) pressure and hybrid vertical coordinates for AGCMs as introduced by ?~~Eq. 5 has been used.

2.2 The stationary case

This scheme assumes that the velocity and pressure fields are in steady state and was introduced by **?** and used and developed for ocean mass transport studies by **?**. The velocity inside a grid cell is found by assuming that it is only a function of its direction, i.e. $u = u(x), v = v(y), w = w(z)$. Linear interpolation gives the zonal velocity

$$u(x) = u_{i-1,j,k} + \frac{x - x_{i-1}}{\Delta x}(u_{i,j,k} - u_{i-1,j,k})\cancel{.}, \tag{16}$$

~~We know that~~ and similarly for $v(y)$ and $w(z)$. To calculate the zonal position, x, of a trajectory, we use $u = dx/dt$, and ~~can write this~~ write Eq. 16 as the differential equation

$$\frac{dx}{dt} - \cancel{x}\frac{u_i - u_{i-1}}{\Delta x}x + \frac{x_{i-1}}{\Delta x}(u_i - u_{i-1}) - u_{i-1} = 0.$$

If we now substitute x for a non-dimensional position $\cancel{r = x/\Delta x}$ $r \equiv x/\Delta x$ and t for a scaled time $s \equiv t/(\Delta x_{i,j}\Delta y_{i,j}\Delta z_k)$, we get

$$\frac{dr}{ds} + \beta r + \delta = 0\,, \tag{17}$$

where $F = dr/ds$ is the zonal volume or mass flux, and $\beta \equiv F_{i-1,j,k} - F_{i,j,k}$ and $\delta \equiv -F_{i-1,j,k} - \beta r_{i-1}$ are constants. Its solution describes the zonal displacement within the grid box between the ~~walls~~ faces and is found using the initial condition $r(s_0) = r_0$ of its zonal position so that

$$r(s) = \left(r_0 + \frac{\delta}{\beta}\right)e^{-\beta(s - s_0)} - \frac{\delta}{\beta}\,. \tag{18}$$

The scaled time s_1 becomes

$$s_1 = s_0 - \frac{1}{\beta}\log\left[\frac{r_1 + \delta/\beta}{r_0 + \delta/\beta}\right]\,, \tag{19}$$

where $r_1 = r(s_1)$ is given by either r_{i-1} or r_i, when a trajectory enters the western or eastern ~~wall~~grid face, respectively. The logarithmic factor in Eq. (~~1~~19) can be expressed as $\log[F(r_1)/F(r_0)]$.

For a trajectory reaching the ~~wall~~ grid face $r = r_i$ ~~, for instance, the transport~~ or $r = r_{i-1}$ both $F(r_1)$ ~~must necessarily be positive, so~~ and $F(r_0)$ must be of the same sign in order for Eq. (19) to have a solution~~, the transport .~~. If $F(r_1)$ and $F(r_0)$ ~~must also be positive. If this is not the case, then the trajectory either reaches the opposite wall at r_{i-1} or the signs of the transports are such that~~ are of opposite signs there is a zero zonal transport ~~somewhere inside the grid box, which~~ at a position between r_1 and r_0 and this position is reached exponentially ~~slowly~~slow.

The ~~calculations of~~ above procedure is repeated for meridional and vertical displacements, where now $r = y/\Delta y$ or $r = z/\Delta z$. This yields non-dimensional position, r_1, and scaled time, s_1 ~~are performed determining~~, for the zonal, meridional and vertical displacements of the trajectory, respectively, inside the grid box under consideration. The smallest transit time $s_1 - s_0$ and the corresponding r_1 denote through which ~~wall~~ grid face of the grid box the trajectory will exit and move into the adjacent one. The exact displacements in the other two directions are then computed using the smallest s_1 in the corresponding Eq. (18).

~~The solutions in the meridional and vertical directions are calculated similarly as the zonal one but using the meridional and vertical transports, respectively.~~

Note that Eqs. (18)-(19) are not valid if the transport fields across the grid box are constant, i.e. when $(F_{i-1,j,k} = F_{i,j,k})$, since it would imply a division by zero with $\beta = 0$ in both equations. The differential equation then simplifies to

$$\frac{dr}{ds} + \delta = 0\,, \tag{20}$$

which has the solution

$$r(s) = -\delta\,(s - s_0) + r_0, \tag{21}$$

and the scaled time s_1 is

$$s_1 = s_0 - \frac{r_1 - r_0}{\delta}\,. \tag{22}$$

~~The solution above allows Δz to vary in space and time. Hence, TRACMASS works for any generalised vertical coordinate system, e. g. z, z^*, $\tilde{z}$, or σ. **?** used TRACMASS with ERA-Interim reanalysis, which uses terrain-following hybrid coordinates.~~ If $F_{i-1,j,k} = F_{i,j,k}$, TRACMASS instead uses Eq. 21, 22.

2.3 "Stepwise-stationary" and "Fixed GCM time step" integrations

The trajectory scheme above is, strictly speaking, only valid for stationary fields. The scheme is, however, possible to use for time-dependent fields by assuming that the velocity and surface-elevation fields are stationary during a limited time interval. The "stepwise-stationary" method presented here consists of assuming that the fields are stationary during intermediate time steps between two GCM outputs and then updated successively as new fields become available. If this is undertaken "on-line", i.e., in the same time as the GCM is integrated, this time interval will simply be the same as the time step the GCM is integrated with, which is typically of the order of minutes in a global GCM. If instead the trajectories are calculated "off-line", the time interval between GCM fields will be at least as often as the fields have been stored by the GCM, at intervals that can be days or even months.

A linear time interpolation of the velocity fields between two GCM velocity fields permits a simple way to have shorter time steps by which the fields are updated in time. The time interval between two GCM velocity fields is Δt_G and the shorter time interval at which the fields are interpolated is Δt_i as illustrated by Fig. 1. The number of intermediate time steps is hence the ratio $I_S = \Delta t_G / \Delta t_i$. For any quantity in the GCM output, F, the value at intermediate time step m, located between GCM outputs $n-1$ and n, is

$$F(t^m) \equiv F^m = \frac{t^m - t^{n-1}}{\Delta t_G}(F^n - F^{n-1}) + F^{n-1}\,. \tag{23}$$

The coefficients β, δ in Eq. (17) are updated when a trajectory moves from one grid box to another. Thus, the time step for the trajectory, i.e. $s_1 - s_0$, may be shorter than the intermediate time step, Δt. Δt_i is hence the maximum possible time step for a given I_S, but is often shorter if the spatial resolution (Δx, Δy, Δz) is small and Δt_G long. We will therefore test TRACMASS by imposing constant velocities for the entire Δt_G in order to mimic other codes such as the Ariane code based on **?**, which do not make any temporal interpolations of the velocity fields. This particular case of the "stepwise-stationary" scheme with constant velocity fields for the entire period between two GCM outputs will be denoted the "fixed GCM time step". These two schemes together with a truly time dependent scheme, described in next section, will be tested.

2.4 Analytical time integration with the "time-dependent" scheme

The "stepwise-stationary" integration method presented in the previous section assumes that the velocity and the grid box thicknesses remain constant throughout the time step, and only spatial variations of velocity are accounted for. Another approach is to interpolate the velocity fields, not only in space within the grid box, but also in time between the GCM outputs. This approach, introduced in TRACMASS by **?**, is more accurate but involves a more advanced differential equation to be solved and integrated along the trajectories. Accounting for both spatial and temporal variations of velocities in the trajectory scheme render intermediate time steps unnecessary. We will later show that using a large number of intermediate steps, the "stepwise-stationary" scheme approaches this "time-dependent" scheme asymptotically.

The "time-dependent" scheme can be derived in the same way as Eq. 17, but instead of a linear interpolation in space, we use a ~~bi-linear~~ bilinear interpolation in both space and time. As before, we use non-dimensional position $r = x/\Delta x$, and scaled time $s \equiv t/(\Delta x \Delta y \Delta z)$, where the denominator is the volume of the particular grid box. For a zonal volume or mass flux F a ~~bi-linear~~ bilinear interpolation in space and time yields

$$\begin{aligned} F(r,s) &= F_{i-1}^{n-1} + (r - r_{i-1})(F_i^{n-1} - F_{i-1}^{n-1}) + \\ & \quad + \frac{s - s^{n-1}}{\Delta s}\left[F_{\cancel{i-1,n}\,i-1}{}^{n} - F_{i-1}^{n-1} + (r - r_{i-1})(F_i^n - F_{i-1}^n - F_i^{n-1} + F_{i-1}^{n-1})\right], \end{aligned} \tag{24}$$

Δs is the scaled time step between two data sets:

$$\Delta s = s^n - s^{n-1} = (t^n - t^{n-1})/(\Delta x \Delta y \Delta z) = \Delta t_G/(\Delta x \Delta y \Delta z)\,, \tag{25}$$

where Δt_G is the time step between two data sets in true time dimension (seconds). Similar expressions for the meridional and vertical directions can be derived.

Connecting the local transport to the time derivative of the position with $F = dr/ds$, the following differential equation is obtained:

$$\frac{dr}{ds} + \alpha\, r\, s + \beta\, r + \gamma\, s + \delta = 0\,, \tag{26}$$

where the coefficients are defined by

$$\alpha \equiv -\frac{1}{\Delta s}(F_i^n - F_{i-1}^n - F_i^{n-1} + F_{i-1}^{n-1}), \tag{27}$$

$$\beta \equiv F_{i-1}^{n-1} - F_i^{n-1} - \alpha s^{n-1}, \tag{28}$$

$$\gamma \equiv -\frac{1}{\Delta s}(F_{i-1}^n - F_{i-1}^{n-1}) - \alpha r_{i-1}, \tag{29}$$

$$\delta \equiv -F_{i-1}^{n-1} + r_{i-1}(F_i^{n-1} - F_{i-1}^{n-1}) - \gamma s^{n-1}. \tag{30}$$

Different analytical solutions exist for the three cases: $\alpha > 0$, $\alpha < 0$ and $\alpha = 0$, which together cover all possible values of α. The acceleration, inside the $r - s$ grid box, is $d^2r/ds^2 = -\alpha r - \gamma$, which is constrained by a linear r-dependent term proportional to α and the constant γ.

2.4.1 The case $\alpha > 0$

For this case, we define the time-like variable $\xi = (\beta + \alpha s)/\sqrt{2\alpha}$ and get

$$r(s) = \left(r_0 + \frac{\gamma}{\alpha}\right) e^{\xi_0^2 - \xi^2} - \frac{\gamma}{\alpha} + \frac{\beta\gamma - \alpha\delta}{\alpha}\sqrt{\frac{2}{\alpha}}\left[D(\xi) - e^{\xi_0^2 - \xi^2} D(\xi_0)\right], \tag{31}$$

where Dawson's integral

$$D(\xi) \equiv e^{-\xi^2} \int\limits_0^{\xi} e^{x^2} dx \tag{32}$$

has been used, as well as, the initial condition $r(s_0) = r_0$. An example of trajectories in this case is illustrated in Fig. 2a, with given values of F_{i-1}^{n-1}, F_i^{n-1}, F_i^n and F_{i-1}^n. We see here that $\alpha > 0$ occurs when the flow changes from divergence in the i-direction at time step $n-1$ to convergence at time step n.

2.4.2 The case $\alpha < 0$

When $\alpha < 0$, ξ becomes imaginary. By defining $\zeta \equiv i\xi = (\beta + \alpha s)/\sqrt{-2\alpha}$, Eq. (31) can be re-expressed as

$$r(s) = \left(r_0 + \frac{\gamma}{\alpha}\right) e^{\zeta^2 - \zeta_0^2} - \frac{\gamma}{\alpha} - \frac{\beta\gamma - \alpha\delta}{\alpha}\sqrt{\frac{\pi}{-2\alpha}}\, e^{\zeta^2}\left[\mathrm{erf}(\zeta) - \mathrm{erf}(\zeta_0)\right], \tag{33}$$

where the error function $\mathrm{erf}(\zeta) = (2/\sqrt{(\pi)}\int_0^{\zeta} e^{-x^2} dx$. An example of trajectories for this case is illustrated in Fig. 2b. We see here that $\alpha < 0$ occurs when the flow changes from convergence in the i-direction at time step $n-1$ to divergence at time step n.

2.4.3 The case $\alpha = 0$

The solution of Eq. (26) when $\alpha = 0$ is

$$r(s) = \left(r_0 + \frac{\delta}{\beta}\right) e^{-\beta(s-s_0)} - \frac{\delta}{\beta} + \frac{\gamma}{\beta^2}\left[1 - \beta s + (\beta s_0 - 1)e^{-\beta(s-s_0)}\right]. \tag{34}$$

This case would normally not occur in a realistic GCM integration, but if for some reason such as a chosen constant field in time or space, α will be zero, since $F_i^n - F_{i-1}^n = F_i^{n-1} + F_{i-1}^{n-1}$. Note that if the fields are in steady state, Eq. (34) is reduced to become identical to the stationary solution of Eq. (18). An example of trajectories in this stationary case is illustrated in Fig. 2c.

If instead $\alpha = 0$ since the fields are constant in space, i.e. the transport across the grid cell is constant ($F_i = F_{i-1}$), then we also have $\beta = 0$, which leads to a simplification of Eq. (26):

$$\frac{dr}{ds} + \gamma s + \delta = 0\,, \tag{35}$$

with the solution

$$r(s) = r_0 - \frac{\gamma}{2}\left(s^2 - s_0^2\right) - \delta\,(s - s_0)\,. \tag{36}$$

An example of trajectories in this case with constant fields in space is illustrated in Fig. 2d.

2.5 The transit time

A major difference ~~with~~ between the "time-dependent" and the "stepwise-stationary" ~~method (solution of Eq. (18))~~ schemes is that the transit times $s_1 - s_0$ cannot in general be obtained explicitly ~~.~~ with the "time-dependent" scheme in contrast to the "stepwise-stationary" analytical solution of Eq. (18). Using the solutions given by Eqs. (31)–(34), the relevant root s_1 of

$$r(s_1) - r_1 = 0 \tag{37}$$

has to be computed numerically for each direction. ~~In the following subsection, we~~ We will now describe how the roots s_1 and the corresponding exiting ~~wall~~ grid face r_1 can be determined. The displacement of the trajectory inside the grid box under consideration then proceeds as previously discussed for stationary velocity fields.

We now determine the roots s_1 of Eq. (37) and the corresponding r_1 needed to calculate trajectories inside a grid box. In what follows, $s^{n-1} \leqslant s_0 < s^n$ and the relevant roots s_1 are to be in the interval of $s_0 < s_1 \leqslant s^n$. We also focus on the cases $\alpha > 0$ and $\alpha < 0$, since the forthcoming considerations can easily be adapted for the case of $\alpha = 0$. For numerical purposes, we use

$$\frac{\beta\gamma - \alpha\delta}{\alpha} = \cancel{\frac{F_{i,n}F_{i-1}^{n-1} - F_i^{n-1}F_{i-1}^n}{F_i^n - F_{i-1}^n - F_i^{n-1} + F_{i-1}^{n-1}}}\; \frac{F_i^n F_{i-1}^{n-1} - F_i^{n-1}F_{i-1}^n}{F_i^n - F_{i-1}^n - F_i^{n-1} + F_{i-1}^{n-1}}\,, \tag{38}$$

$$\frac{\gamma}{\alpha} = \frac{F_{i-1}^n - F_{i-1}^{n-1}}{F_i^n - F_{i-1}^n - F_i^{n-1} + F_{i-1}^{n-1}} - r_{i-1}\,, \tag{39}$$

$$\xi = \frac{F_{i-1}^{n-1} - F_i^{n-1} + \alpha(s - s^{n-1})}{\sqrt{2\alpha}}\,, \tag{40}$$

$$\zeta = \frac{F_{i-1}^{n-1} - F_i^{n-1} + \alpha(s - s^{n-1})}{\sqrt{-2\alpha}}\,. \tag{41}$$

As above, s is the scaled time. The coefficient in Eq. (38) appearing in Eqs. (31) and (33) is exactly zero when either the r_{i-1} or r_i ~~wall~~ grid face represents a solid boundary, so that transport F_i or F_{i-1} is zero for all n, respectively. In these instances, the opposite ~~wall~~ grid face fixes r_1 , and the root $s_1 > s_0$ can be computed analytically. If there is no solution, we take $s_1 = s^n$. When all three transit times equal s^n, the trajectory will not move into an adjacent grid box but will remain inside the original one. Its new position is subsequently determined, and the next time interval is considered.

The roots of Eq. (37) have to be computed numerically if $(\beta\gamma - \alpha\delta)/\alpha \neq 0$. This is also true for locating the extrema of the solutions given by Eqs. (31) and (33). Alternatively, one can consider the case $F(r,s) = 0$ using Eq. (24) to analyse where possible extrema are located. It follows that in the s-r-plane, the extrema lie on a hyperbola of the form $r = (as+b)/(c+ds)$. Obviously, only the parts defined by $s^{n-1} \leq s \leq s^n$ and $r_{i-1} \leq r \leq r_i$ are relevant. Depending on which parts of the hyperbola, if any, lie in this "box" and satisfy the initial condition $r(s_0) = r_0$, the trajectory $r(s)$ exhibits none, one, or at most two extrema. In the latter case, the trajectory will not cross either the ~~wall~~ grid face at r_{i-1} or the one at r_i (see Fig. 2 for an example). Hence, the trajectories $r(s)$ determining the transit time $s_1 - s_0$ will have at most one extremum, i.e., there is at most one change of sign in the local transport F.

An efficient way of proceeding is as follows: first consider the ~~wall~~ grid face at r_i. For a trajectory to reach this ~~wall~~grid face, the local transport must be nonnegative, which depends on the signs of the transport ~~$F_{i-1,n}$ and $F_{i,n}$~~F^n_{i-1} and F^n_i. Four distinct configurations may arise between the model outputs ($s^{n-1} < s < s^n$), where the calculation of the trajectory takes place:

1. $F(r_i, s) > 0$ for $s^{n-1} < s < s^n$.

2. The sign of $F(r_i, s)$ changes from positive to negative at $s = s^*$, where $s^{n-1} < s^* < s^n$

3. The sign of $F(r_i, s)$ changes from negative to positive at $s = s^\#$, where $s^{n-1} < s^\# < s^n$.

4. $F(r_i, s) < 0$ for $s^{n-1} < s < s^n$.

These four cases are illustrated by the four panels of Fig. 3.

For case 1, we evaluate $r(s^n)$ using the appropriate analytical solution. If, in addition $r(s^n) \geq r_i$, then the trajectory has crossed the grid-box ~~wall~~ face $r = r_i$ at $s_1 \leq s^n$ as shown by the trajectories A, B and C in Fig. 3. If the initial transport $F(r_0, s_0) < 0$, the trajectory may have crossed the opposite ~~wall~~ grid face at an earlier time as illustrated by trajectory C in Fig. 3. This is only possible if case 3 applies for the ~~wall~~ grid face at r_{i-1} and $s^\# > s_0$, in which case it is determined whether $r(s^\#) \leq r_{i-1}$. If this is not the case, there is a solution to $r(s_1) - r_1 = 0$ for $r_1 = r_i$ and $s_0 < s_1 \leq s^n$. Subsequently, this root can be calculated numerically using a root-solving algorithm (?). But if $r(s^n) < r_i$ or, if applicable, $r(s^\#) \leq r_{i-1}$, we proceed by considering the other ~~walls~~grid faces. The arguments for the ~~wall~~ grid face at r_{i-1} are similar to those relating to ~~r~~r_i.

If case 2 applies and $s_0 < s^*$, we add here to the considerations given in case 1 using s^* instead of s^n. If there is a root for $r_1 = r_i$, then $s_0 < s_1 \leq s^*$. This root is illustrated by trajectory D in Fig. 3 with $(r_1, s_1) = (r_i, s_{1D})$.

For case 3, we follow the procedure given by case 1. If there is a root for $r_1 = r_i$, then $s^\# < s_1 \leq s^n$. This root is illustrated by trajectory E in Fig. 3 with $(r_1, s_1) = (r_i, s_{1E})$.

For case 4, no solution of Eq. (37) is possible for $r_1 = r_i$, since all trajectories exit through the ~~wall~~ grid face located at r_{i-1} as illustrated by trajectory G in Fig. 3 or will not reach any ~~wall~~ grid face during the time interval $s^{n-1} < s < s^n$. We must then instead search for an exit through another of the six ~~walls~~grid faces.

All these considerations are applied to each of the three spatial directions in order to determine through which of the 6 ~~grid-box walls~~ grid faces the trajectory will exit and at which position on the corresponding ~~wall~~grid face.

Since the trajectories are unique solutions to Eq. 26 and the continuity equation is respected, the TRACMASS trajectories will therefore never hit any solid boundary such as the coast or the sea floor unless the sedimentation option is activated, where an extra velocity is imposed, a feature that was introduced in TRACMASS by **?**.

An example of the evolution of trajectories calculated with the three different schemes within a time-space cell for $\alpha > 0$ is shown in Fig. **??**. The trajectories computed with the "stepwise-stationary" scheme approaches the trajectory computed with the "time-dependent" with increasing number of intermediate time steps (I_S). The "fixed GCM time step" trajectory can, however, not follow the "time-dependent" one since it does not update the velocities between the GCM outputs and consequently deviates immediately as it leaves the initial point (r_0, s^{n-1}).

3 Tests with different velocity fields

The results obtained from the "stepwise-stationary" scheme are now compared with those from the "time-dependent" trajectory schemes using two different sets of velocity fields. The first uses an eddy-resolving OGCM with z-star coordinates. The second uses a global Atmospheric General Circulation Model with hybrid pressure coordinates. For the "stepwise-stationary" scheme, five different settings of I_S, i.e. the number of intermediate steps, are tested. The "fixed GCM time step" is also tested for comparison, although it is not a standard feature of TRACMASS.

3.1 Ocean trajectories with an Eddy resolving OGCM

Oceanic velocity fields for this case were obtained from a simulation with the 3.6 version of the NEMO ocean model (**?**) in a global ORCA12 configuration. The horizontal resolution of the ORCA12 grid is approximately $1/12°$, corresponding to $\Delta x \approx 6$ km at $50°$ latitude. Model fields were available as 5-day averages every 5 days. The configuration uses 75 z^* vertical levels with partial bottom cells, where Δz ranges from ~ 1 m at the surface to 250 m in the deepest parts of the ocean. The z^* coordinate approach permits large-amplitude free-surface variations relative to the vertical resolution (**?**). In the z^* formulation, the variation of the column thickness due to sea-surface undulations is not concentrated to the surface level, as in the z-coordinate formulation, but is equally distributed over the full water column. Thus the vertical levels naturally follow the sea-surface variations, which also implies ~~the~~ that they are time dependent and we therefore have used Eq. (12) to calculate the vertical transport in TRACMASS with a time dependent Δz^n in the equation. The model was forced with 6-hourly atmospheric fields from what is known as the Drakkar Forcing Set, version 4 (DFS4) (**?**). Sub-grid processes were represented using 125 $\mathrm{m}^2\,\mathrm{s}^{-1}$ Laplacian iso-neutral tracer diffusion, and $-1.25 \cdot 10^{10}$ $\mathrm{m}^4\,\mathrm{s}^{-1}$ bi-Laplacian viscosity.

TRACMASS has been applied to this specific model integration already by **?**, where it was compared with surface drifters in the Agulhas region. This is also the region where we are going to test TRACMASS because of its complex time-dependent dynamics with travelling eddies, known as "Agulhas rings", which "leak" Indian-Ocean water into the Atlantic Ocean as part of the Conveyor Belt. 2193 trajectories were started, evenly spread over 4 grid ~~boxes~~ horizontal boxes at all depths in the Indian Ocean, and followed for 50 days as shown in ~~Fig. 4~~ Figs. 4 and 5.

3.2 Atmospheric trajectories with an AGCM

In order to test the trajectory schemes in the atmosphere we have used the ERA-Interim reanalysis (**?**) from the European Centre for Medium-range Weather Forecasts (ECMWF) simulated with the IFS (Integrated Forecasting System) model. In this ERA-Interim data set, the vertical coordinate is a terrain-following hybrid coordinate (**?**), where the pressure at the lower interface of level k is given by $p_k = A_k + B_k p_s$, where p_s is the surface pressure and A_k and B_k are parameters at the level $k \in [0, 60]$, with $p_{60} = p_s$ and $p_0 = 0$. As in the NEMO ocean model, the grid cell thickness varies in time, and we calculate vertical mass flux from the continuity equation (Eq. 15). The ERA-Interim data used here had a horizontal resolution of $1.25°$ and is available 6-hourly (Δt_G). Trajectories are shown in Fig. 6. They were initiated every 6 hours from a grid cell air column over Eyjafjallajökull Volcano eruption during 14-18 March 2010. The trajectories were evenly distributed horizontally and started in exactly same positions for the tests with different time steps using the "stepwise-stationary" scheme and "time-dependent" case.

3.3 Lagrangian statistics

The average distance between the trajectories obtained with the "time-dependent" scheme and the five different "stepwise-stationary" cases as well as the "fixed GCM time step" case are shown in Fig. 7. The distances from the "time-dependent" trajectories after 50 days for the OGCM case and after 10 days for the AGCM case are presented in Table 1. These average distances have been ~~been~~ possible to compute since of all the individual trajectories were started in the exact same positions for the different cases. Results clearly show that the distance between trajectories calculated with the "stepwise-stationary" scheme and those calculated with the "time-dependent" scheme decreased as the number of intermediate time steps were increased. The "fixed GCM time step" case, i.e. when no intermediate time steps are used, shows the greatest distance to the "time-dependent" case.

Standard Lagrangian statistics have also been computed for the ocean trajectories (Fig. 8), with the definitions given in the Appendix. The *relative* and *absolute dispersion* as well as the *mean displacement* of the trajectory cluster show how the cluster will disperse and move in time. They reveal a similar pattern, where only the "fixed GCM time step" case differs from the others. The "fixed GCM time step" differs already after 3 to 4 days, which should be related to the fact that the GCM velocities are updated every 5 days ($= \Delta t_G$) in this OGCM case.

The *Lagrangian velocity autocorrelation*, which describes the correlation of the velocity of the trajectories at one time with that of previous times, shows in Fig. 8 how all cases except the "fixed GCM time step" give nearly the exact same correlation. The Lagrangian time scale, which is computed from the autocorrelation and is a measure of the memory of the trajectories, reflects the same feature with a Lagrangian time scale of approximately 3.9 days for the "time step" and the "time-dependent" cases but a slightly shorter time scale of 3.4 days for the "fixed GCM time step" case. The Lagrangian time scale based on observations with surface drifters is clearly shorter than this both for the Global Ocean (?) and in the Agulhas region (?). This relatively shorter Lagrangian time scale (hence closer to observations for the "fixed GCM time step") is simply due to the abrupt changes in the velocity fields every time these are updated. A realistic shortening of the Lagrangian time scale can only be obtained by incorporating finer scales by increasing the GCM resolution or adding sub-grid parameterisations to the trajectories.

The power spectra computed from the Lagrangian velocities show that the "fixed GCM time step" was more energetic than the other schemes, which all yielded nearly identical results. This is the case for all frequencies. There is also a weak maximum at 4 cycles/day (6 hours), which remains unexplained, although it may be related to the fact that the OGCM uses 6-hourly atmospheric forcing.

3.4 Lagrangian stream function and residence time

The mass conservation properties of the used trajectory schemes make it possible to calculate mass transports between different sections in the model domain (?). The approach is that one can associate each trajectory particle with a mass or volume transport. This requires that enough trajectories are computed to fill the model grid in space and time with a sufficient number of trajectories. Lagrangian stream functions can be calculated by summing over trajectories representing a desired path (???). The difference between the "Lagrangian" and the more common "Eulerian" stream functions is that with the Lagrangian one can isolate a particular path between a starting and an ending section in the ocean or the atmosphere.

~~We have here computed the barotropic Lagrangian stream function from the released particles. The top left panel of Fig. 9 shows this computed with the "time-dependent" trajectory scheme. In order to measure the differences due to the the~~ The influence of the the different trajectory schemes ~~, we have subtracted the stream function obtained from~~ on the inter-ocean exchange of water masses, which takes place in the Agulhas region, has been evaluated by calculating Lagrangian stream functions. Fig. 9 shows the Lagrangian barotropic stream function computed from trajectories using the "time-dependent" ~~trajectories from those integrated with~~ scheme and the "~~stepwise-stationary" and "~~fixed GCM time step" ~~trajectories (Fig. 9) . It is only the~~ scheme. Lagrangian decomposition has been used to compute two separate stream functions for each scheme, one from trajectories entering the Atlantic and one from those returning back into the Indian Ocean via the Agulhas retroflection region. The "time-dependent" scheme favours slightly (one additional stream line) the entering into the Atlantic compared to the "fixed GCM time step" ~~stream function that clearly deviates. The total transport between the different basins will, however, not differ much between the schemes.~~ scheme. This is also clearly visible when computing the residence time, i.e. the time ~~a trajectory stays~~ trajectories stay within the Agulhas region ~~. We have also computed the total amount of trajectories remaining in the Agulhas region as a function of time as~~ as shown in the lower righthand panel of Fig. 8. ~~We have also decomposed whether the particles exit the region into the Atlantic or Indian Ocean.~~ The first particles start to exit the Agulhas region as defined by the map in Fig 9 after 50 days. The number of trajectory particles then decays exponentially with an e-folding time of about 210 days. This is rather similar for all trajectory-scheme integrations. There is, however a clear difference in the results where the trajectories exit. The "fixed GCM time step" scheme results in 38 % flowing into the Atlantic and 59 % into the Indian Ocean after 800 days. All the other trajectory integrations yield very similar results but with 46 % flowing into the Atlantic and 52 % into the Indian Ocean. This suggests that the "fixed GCM time step" scheme does not capture the same behaviour as the other schemes.

We have repeated the above ocean-trajectory experiment by releasing the particles in other time periods and increasing the ensemble size. The results only changed marginally.

3.5 Computational speed

In addition to the higher accuracy of the "time-dependent" scheme, it was also shown to be computationally faster than the "stepwise-stationary" scheme with intermediate time steps. In order to quantify this we compared the computational time for the different schemes using analytical velocity fields describing inertia oscillations (**?**), where no data needed to be read nor written since the velocity fields have a known analytical solution and disk storage was switched off. These computational times are shown in the last column of Table 1, which have been normalised by dividing with the time obtained with the "time-dependent" scheme. The "stepwise-stationary" scheme was only as computationally fast as the "time-dependent" scheme when no extra intermediate time steps were taken between two readings of the velocity fields ($I_S = 1$) or when using "fixed GCM time steps". When the number of intermediate time steps was increased to $12,000$, the "stepwise-stationary" scheme was more than 1000 times slower. $12,000$ intermediate steps was also approximately the number of intermediate time steps required in order to obtain as accurate results as those obtained from the "time-dependent" scheme.

4 Discussion and Conclusions

The two trajectory schemes available in TRACMASS have here been inter-compared by calculating Lagrangian statistics, transports and the distances between the trajectories. This has been done for both oceanic and atmospheric applications. The "stepwise-stationary" scheme assumed that the velocity fields were stationary for ~~some time~~ the duration of a user defined intermediate time step between model output fields. These velocities are, however updated with a linear interpolation in time when crossing a model grid ~~wall~~face. The "time-dependent" scheme does not assume that the velocity is in steady state during any time interval since it solves the differential equations of the trajectory path not only in space but also in time. This continuous evolution of the "time-dependent" scheme makes it more accurate than the "stepwise-stationary" scheme without any significant increase in computational expense.

In addition to these two TRACMASS schemes, we have ~~used~~ tested a "fixed GCM time step" scheme, which is in fact a special case of the "stepwise-stationary" scheme but with velocity fields always remaining in steady state until a new GCM data set is reloaded in order to mimic the Ariane trajectory model (**?**). A consequence of only updating the fields at the GCM output times is that the velocities are assumed to be in steady state for long periods and then changed abruptly with a discontinuity.

The accuracy of the schemes has been evaluated by comparing the distance between particles that have been started from the same positions but with different trajectory schemes, and how this distance evolves in time. This distance was shown to depend on the scheme and the number of intermediate time steps for the "stepwise-stationary" case. The average distance as a function of time between the trajectories obtained from the different schemes are shown in Fig. 7 as well as their end position distances in Table 1.

The study has shown that the TRACMASS "time-dependent" scheme is both more accurate and faster than the "stepwise-stationary" scheme with intermediate steps. It remains to be shown how the trajectory schemes used in the present study compare to other trajectory schemes, such as e.g. Runge-Kutta, which could be used where mass conservation is not important.

The "stepwise-stationary" scheme needed up to 12,000 intermediate time steps to give as accurate trajectory paths as the "time-dependent" scheme, which is more than a thousand times as computationally expensive when reading and writing is excluded. The distance between trajectories calculated with the "time-dependent" scheme and those obtained with the "stepwise-stationary" scheme decreased as the number of intermediate time steps is increased. The greatest distance was obtained when no temporal variations between GCM outputs at all were considered, i.e. with the "fixed GCM time step" scheme. We thus conclude that the "time-dependent" scheme is the most accurate of those tested here for two reasons. Firstly for theoretical reasons since the "time-dependent" scheme does not assume stationary velocities during any period of time. Secondly the trajectories computed with the "stepwise-stationary" scheme converge towards those computed with the "time-dependent" scheme for increasing numer of intermediate time steps. A future study could be to calculate trajectories first using fields stored at each GCM time step and second using fields stored at longer time intervals. In the first case, trajectories would be very accurate and could represent a "truth", and the second case could be used to evaluate which scheme is the closest to the "truth".

The Lagrangian statistics such as relative and absolute dispersion as well as Lagrangian velocity autocorrelation functions and power spectra showed almost identical results for the "time-dependent" and the "stepwise-stationary" schemes. The "fixed GCM time step" showed, however, some differences from the other two schemes. E.g. the dispersion after 3-4 days was slightly larger for using a "fixed GCM time step", which might be explained by an abrupt change every time the GCM velocities are updated compared to the smoother transition of the two other schemes. The results show that the "fixed GCM time step" method does not capture the same behaviour of trajectories as the other schemes. The Lagrangian statistics are also clearly affected by the model resolution and the time sampling of the GCM fields (**????**). Future improvements to the TRACMASS model will involve improvements of the sub-grid turbulence parameterisations, which could give more realistic dispersion properties.

The mass conservation of the trajectory schemes in the present study arises from that 1) mass transports across the grid ~~walls~~ faces are used in the same way as in the GCM itself instead of velocities as in most other trajectory schemes, 2) the mass transport is linearly interpolated within the grid box, where there is otherwise no information of the velocity from the GCM and that this enables us to set up a differential equation, which has an analytical solution of the trajectory within the grid box. The different trajectory schemes, although mass conserving, will not yield the same results in terms of transports between different sections. This was tested in the Agulhas experiment, where the "fixed GCM time step" scheme favoured relatively the Agulhas retroflection with more trajectories returning into the Indian compared to the "time-dependent" and "stepwise-stationary" schemes. This can be explained by the delicate path of the Agulhas leakage, which requires an accurate temporal evolution so that particles can be retained in Agulhas rings. This was better achieved by the "time-dependent" and "stepwise-stationary" schemes than by the "fixed GCM time step" scheme.

The TRACMASS trajectory code with corresponding schemes has been improved and become more accurate and user friendly over the years. An outcome of the present study is that we strongly recommend the use of the "time-dependent" scheme based on **?** in favour of the "stepwise-stationary" scheme. We would also like to dissuade the use of the more primitive "fixed GCM time step" scheme, which is used in other trajectory codes since the velocity fields remain stationary for longer periods creating abrupt discontinuities in the velocity fields, and yielding inaccurate solutions. We have here only tested one OGCM and one AGCM simulation, but we speculate that at coarser resolution in both space and time, the differences obtained with the two schemes would increase. However, in non eddying simulations (e.g. 1° ocean models) this may not be true due to the low variability of the flow.

The TRACMASS strict requirement of mass conservation makes it, however, necessary to have complete velocity fields on the original GCM grid in order to use mass or volume transports in and out of each model grid box. This will always be somewhat more demanding than for other trajectory codes, since it requires a total understanding of the various GCM coordinate systems as well as incorporating them in the TRACMASS framework. This state of affairs is in marked contrast to what holds true for various trajectory codes that only require velocity fields with no mass conservation.

5 Code availability

TRACMASS version 6.0 is freely available for research purposes at https://github.com/TRACMASS. In addition, the code is archived at http://dx.doi.org/10.5281/zenodo.34157.

Appendix A: Lagrangian-statistics definitions

The Lagrangian statistics used in the present work (shown in Figs. 7 and 8) are here defined. See e.g. **?** for a detailed derivation.

The *average distance* between the different trajectory calculations as presented in Fig. 7 is defined as

$$D_B^2(t) \equiv \frac{1}{N-1}\frac{1}{M-1}\sum_{n=1\,m=1}^{N}\sum_{i=1}^{2}\left(x^{n}_{i\;i,m}(t) - \hat{x}^{n}_{i\;i,m}(t)\right)^2. \tag{A1}$$

It is hence the distance between the two trajectories ~~$x_i^n(t)$ and $\hat{x}_i^n(t)$~~ $x_{i,m}(t)$ and $\hat{x}_{i,m}(t)$, where t is the time, ~~N~~ M the total number of trajectories of the cluster and i the spatial coordinate index (*i.e.* the zonal, meridional or vertical position of the ~~n~~ m-th trajectory ~~$x_i^n(t)$~~ $x_{i,m}(t)$). The two trajectories ~~$x_i^n(t)$ and $\hat{x}_i^n(t)$~~ $x_{i,m}(t)$ and $\hat{x}_{i,m}(t)$ will have the same initial position ~~$(x_i^n(t_0) = \hat{x}_i^n(t_0))$~~ $(x_{i,m}(t_0) = \hat{x}_{i,m}(t_0))$ but will then evolve differently since different trajectory schemes are used to compute their paths. In the present study, we only consider the horizontal dispersion. The vertical dispersion is, however, an important measure of the vertical mixing in the ocean but beyond the scope of the present study.

The mean position of the trajectory cluster is defined as

$$\overline{x_i(t)} \equiv \frac{1}{N}\frac{1}{M}\sum_{n=1\,m=1}^{N\;\;M} x^{n}_{i\;i,m}(t),. \tag{A2}$$

The *relative dispersion* is defined as the mean-square displacement of the trajectories relative to the time-evolving mean position:

$$D_R^2(t) \equiv \frac{1}{N-1}\frac{1}{M-1}\sum_{n=1}^{N}{}_{m=1}^{M}\sum_{i=1}^{2}\left(x_{i\,i,m}^{n}(t)-\overline{x_i(t)}\right)^2. \tag{A3}$$

The *absolute dispersion* is defined in the same way, but relative to the initial position of the cluster:

$$D_A^2(t) \equiv \frac{1}{N-1}\frac{1}{M-1}\sum_{n=1}^{N}{}_{m=1}^{M}\sum_{i=1}^{2}\left(x_{i\,i,m}^{n}(t)-\overline{x_i(t_0)}\right)^2, \tag{A4}$$

where t_0 is the initial time of the trajectory.

The *mean displacement* is defined as the displacement from the origin as a function of time

$$D_D(t_n) \equiv \frac{1}{N}\frac{1}{M}\sum_{m=1}^{N}\sqrt{\sum_{i=1}^{2}[x_{i,n}(t_n)-x_{i,n}(t_0)]^2}^{M}\sqrt{\sum_{i=1}^{2}[x_{i,m}(t)-x_{i,m}(t_0)]^2}. \tag{A5}$$

The *Lagrangian velocity* is obtained by using a non-centered finite difference:

$$u_{i,m}(t_n{}^n) \equiv \frac{dx_{i,m}(t_n)}{dt}\frac{dx_{i,m}(t^n)}{dt} \approx \frac{x_{i,m}(t_n)-x_{i,m}(t_{n-1})}{t_n-t_{n-1}}\frac{x_{i,m}(t^n)-x_{i,m}(t^{n-1})}{t^n-t^{n-1}}, \tag{A6}$$

~~with the same indices as before~~wihere n is the time level. Similarly, the acceleration was calculated by finite differencing of the velocity:

$$a_{i,m}(t_n{}^n) \equiv \frac{du_{i,m}(t_n)}{dt}\frac{du_{i,m}(t^n)}{dt} \approx \frac{u_{i,m}(t_n)-u_{i,m}(t_{n-1})}{t_n-t_{n-1}}\frac{u_{i,m}(t^n)-u_{i,m}(t^{n-1})}{t^n-t^{n-1}}. \tag{A7}$$

Note how velocity is not defined at the first position, and acceleration is not defined at the first velocity.

The *Lagrangian velocity autocorrelation* describes the correlation of the velocity at one time with that of previous times. The definition is

$$R(\tau) = \frac{\sigma^2(\tau)}{\sigma^2(\tau=0)} \approx R_q = \frac{\sigma_q^2}{\sigma_0^2},(t^q)\frac{(\sigma(t^q))^2}{(\sigma(t^0))^2} \tag{A8}$$

where $\sigma^2(\tau)$ and $\sigma^2(\tau=0)$ are the Lagrangian velocity auto-covariances for time lag τ and no lag, respectively. q is the discrete time step and R_q is the autocorrelation at time step q. $\sigma^2(\tau)$ is defined as

$$\sigma^2(\tau) = \lim_{T\to\infty}\frac{1}{T}\int_0^T \mathbf{u}'(t+\tau)\cdot\mathbf{u}'(t)\,dt \approx (\sigma_q(t^q))^2 \equiv \sum_{i=1}^{2}\frac{1}{N-q-1}\sum_{n=1}^{N-q-1} u'_{i,n\,i}(t^n)\,u'_{i,n+q\,i}(t^{n+q}), \tag{A9}$$

where ~~$u'_{i,n} = u_{i,n} - \overline{u}_i$~~ $u'_i(t^n) = u_i(t^n) - \overline{u}_i$ and $\overline{u}_i$ is a time average of the segment. Note that the total velocity autocovariance is the sum of the zonal and meridional components, $\sigma^2 = \sigma_{i=1}^2 + \sigma_{i=2}^2$.

The *Lagrangian time scale* is defined as

$$T_L = \int_0^\infty R(\tau)\,d\tau. \tag{A10}$$

This is a measure of the *memory* of a trajectory, i.e. the time lag during which the Lagrangian velocity is correlated. When computing this integral, the point where $R(\tau) = 0$ for the first time is used here as upper bound. This truncation is perhaps the most commonly used, due to the often noisy character of the auto-correlation function, $R(\tau)$ for large τ.

Acknowledgements. The authors wish to thank Peter Lundberg for constructive comments. This work has been financially supported by the Bolin Centre for Climate Research and by the Swedish Research Council. Joakim Kjellsson is supported by the UK Natural Environment Research Council grant NE/K012150/1: "Poles apart: why has Antarctic sea ice increased, and why can't coupled climate models reproduce observations?". The GCM integrations and the trajectory computations were performed using resources provided by the Swedish National Infrastructure for Computing (SNIC) at the National Supercomputer Centre at Linköping University (NSC).

Table 1. The table shows the average distance between the "time-dependent" integrated trajectories and the "stepwise-stationary" integrated ones at the end of simulations, which is 50 days for the OGCM and 10 days for the AGCM. I_S is the number of intermediate time steps between two GCM outputs. The "maximum time step" stands for the intermediate time step lengths (Δt_i), which are used in the different trajectory integrations. The last column is the the computational time normalised with regard to the "time-dependent" case, where theoretical velocity fields are used to compute trajectories, i.e. with no data reading or writing.

	Distance to "time dependent"		T_L	Maximum Time step		Normalised
	OGCM	AGCM	AGCM	OGCM	OGCM	computational
I_S	$[km]$	$[km]$	$[days]$	Δt_i	Δt_i	time
"Fixed"	769	4992	3.44	≡5 d	≡6 h	0.830
1	276	3835	3.88	5 d	6 h	0.830
12	242	2971	3.86	10 h	30 min	2.110
120	103	1752	3.86	1 h	3 min	14.03
1,200	28	1079	3.87	6 min	18 s	132.0
12,000	6	1002	3.87	36 s	2 s	1191
Time dependent	0	0	3.87	5 d	6 h	1.000

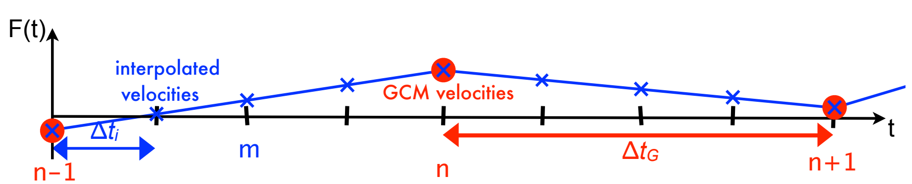

Figure 1. Schematic illustration of how the transport fields $F(t)$ are updated and interpolated in time between the stored GCM data, which are read in at the time t^n and are separated in time by the time interval Δt_G (in red). The fields are then linearly interpolated at the blue points in blue with intermediate time steps. The number of intermediate time steps between two GCM velocities is in this example $I_S = \Delta t_G / \Delta t_i = 4$.

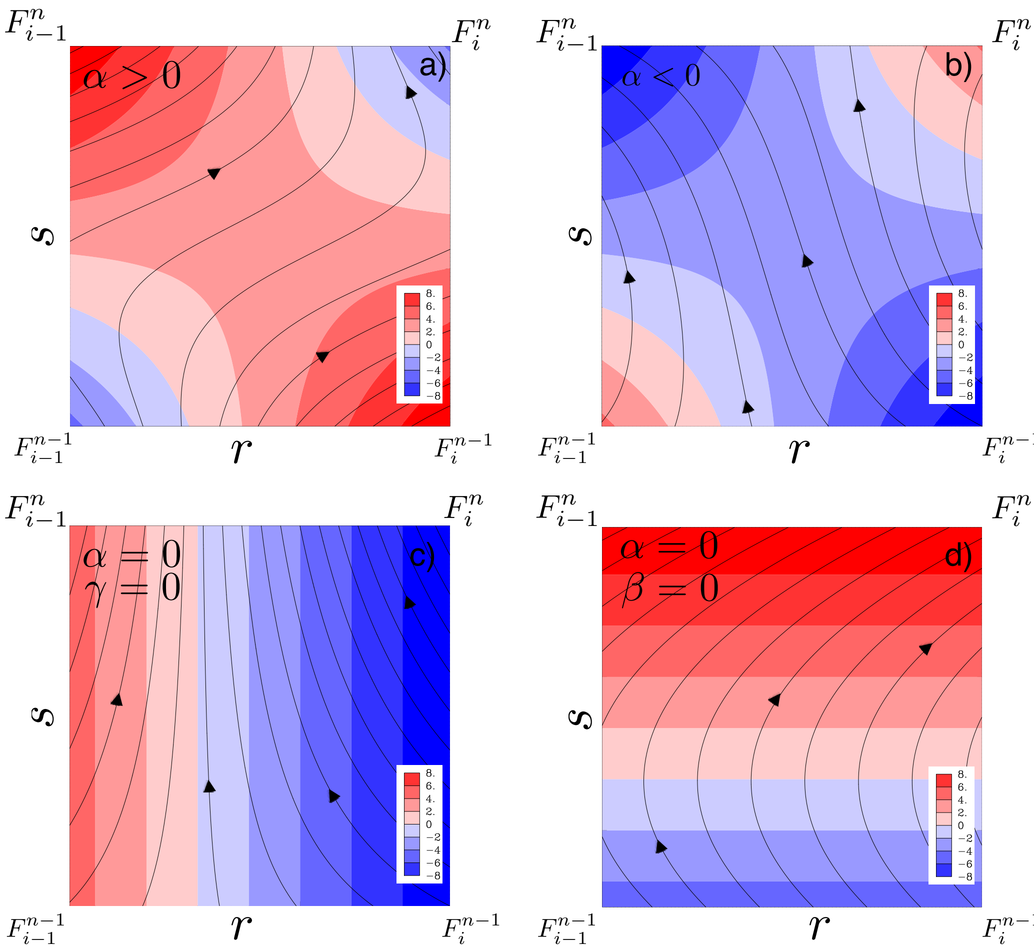

Figure 2. Examples of how trajectories ~~in black would~~ calculated with the "time-dependent" scheme evolve as a function of the transport F in the space interval $r_{i-1} < r < r_i$ and in the time interval $s^{n-1} < s < s^n$, which hence corresponds to an interval between two GCM outputs (Δt_G) and of a grid box (Δx, Δy or Δz). The colour shows the transport values F obtained by the ~~linear~~ bilinear interpolation between the four corners (F^{n-1}_{i-1}, F^{n-1}_i, F^n_i and F^n_{i-1}). a) $\alpha > 0$ with two ~~regions~~ corners of transport in the negative direction ($F < 0$), which correspond to westward, southward or downward directions and one ~~region~~ corner flowing in the opposite direction. b) $\alpha < 0$. c) $\alpha = 0$ and $\gamma = 0$ corresponds to the stationary fields, which results in an ~~F~~ F field that only changes in the the (r) direction. d) $\alpha = 0$ and $\beta = 0$ corresponds to the constant fields in space but which vary in time. Note that the $F = 0$ line between the red and blue colours corresponds to static flow, which results in "vertical" trajectories in the figures.

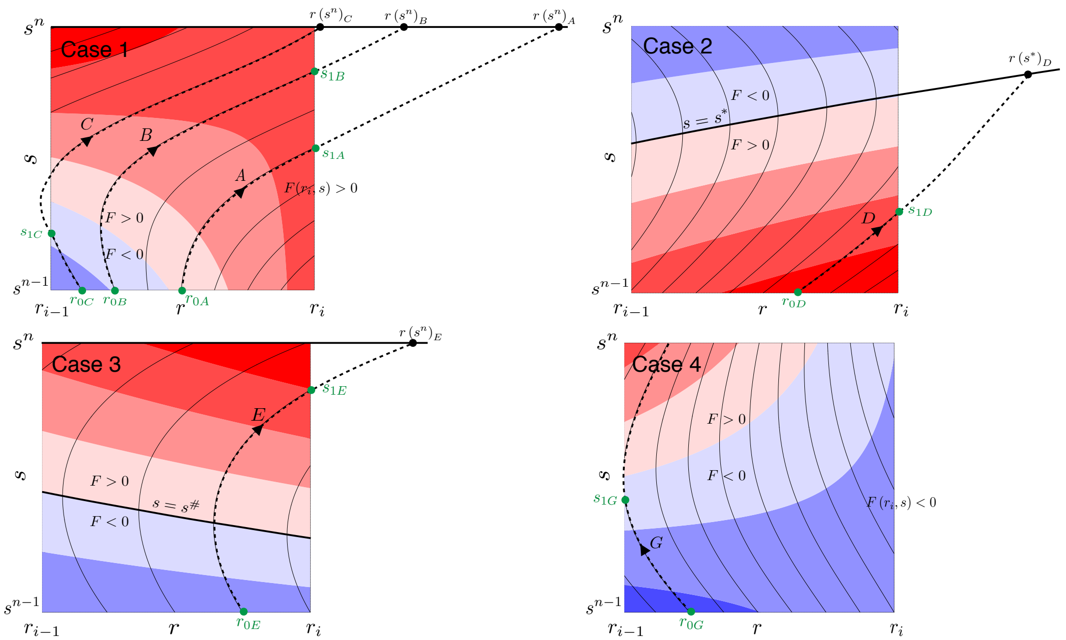

Figure 3. The four different cases of how trajectories might reach the ~~wall~~ grid face at $r = r_i$. Note that the trajectories for case 4 can not reach $r = r_i$. The background colours are the same as in Fig. 2 with $F > 0$ in red and $F < 0$ in blue. The dashed trajectories outside the grid box denote the necessary computed fictive paths for estimating when $s = s_1$ and if the trajectories reach $r_1(s_1) = r_i$.

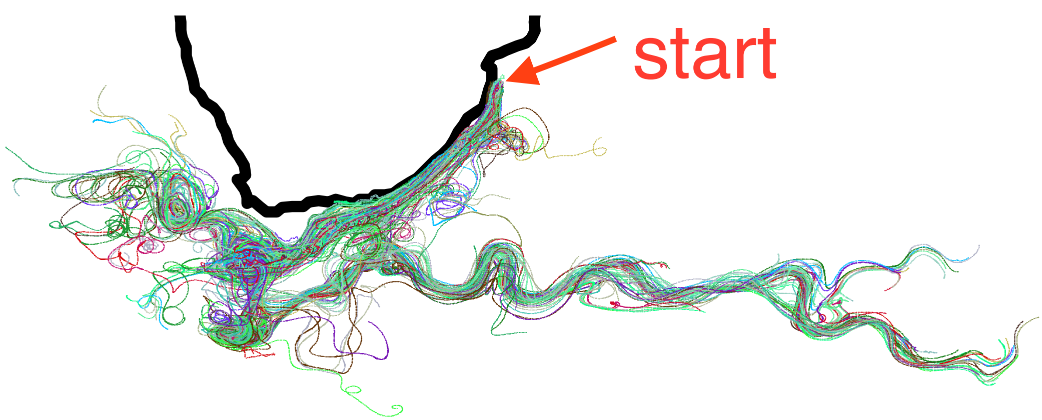

Figure 4. Agulhas trajectories started evenly distributed in a square of 4 grid cells and followed for 50 days. Colouring used to separate the trajectories from each other.

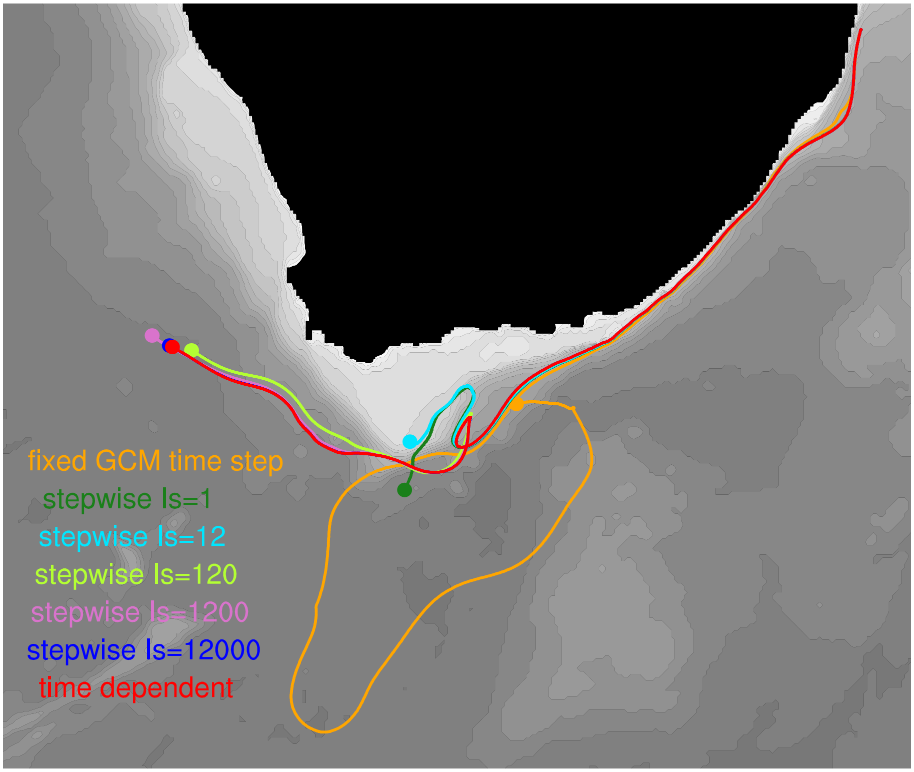

Figure 5. Example of ocean trajectory paths due to different trajectory schemes and number of intermediate time steps. The "time-dependent" method results in red and those obtained with the "stepwise-stationary" method with $I_S = 1, 12, 120, 1200$ and 12000 as well as "fixed GCM time steps". Note that these homologous trajectories were selected to illustrate that "stepwise-stationary" trajectories are closer to "time-dependent" trajectories when the number of intermediate time steps (I_S) is increased.

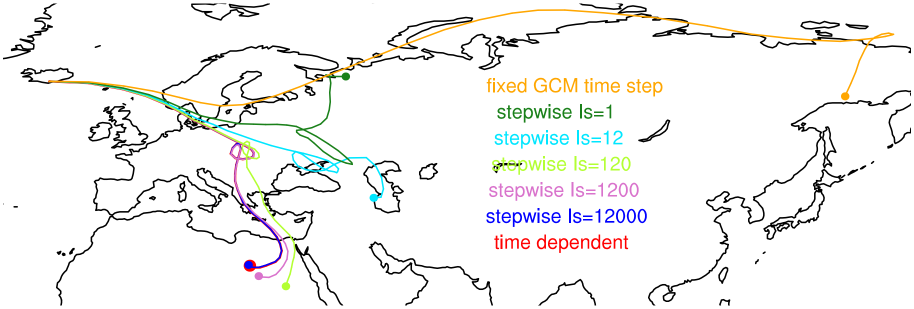

Figure 6. Example of atmospheric trajectory paths starting form the Eyjafjallajökull Volcano during it's eruption calculated with different trajectory schemes and number of intermediate time steps. Same colour coding of the trajectories as in Fig. 5. Note that the red "time-dependent" and the blue "stepwise" with $I_S = 12000$ trajectories are nearly identical.

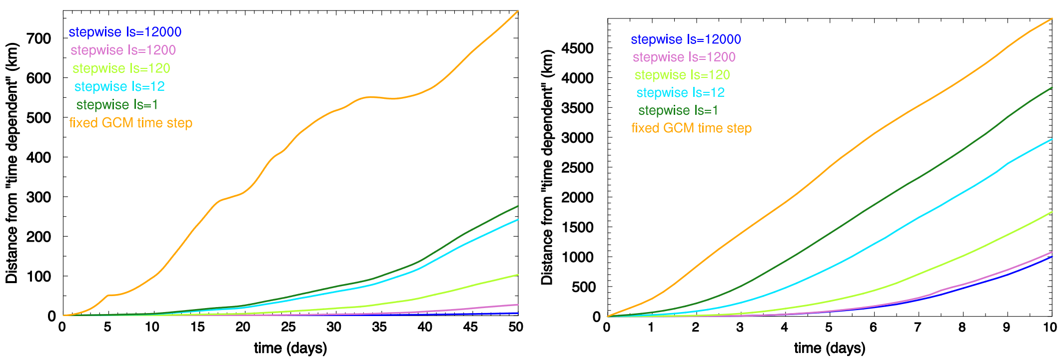

Figure 7. Average distance between the "time-dependent" trajectories and the "stepwise-stationary" ones for the different time-steps with $I_S = 1, 12, 120, 1200$ and 12000 as well as "fixed GCM time steps". The left panel represents the ocean Agulhas trajectories and the right panel the atmospheric ERA-Interim ones. Note that the more intermediate steps used by the "stepwise-stationary" scheme the closer results to the "time-dependent" scheme.

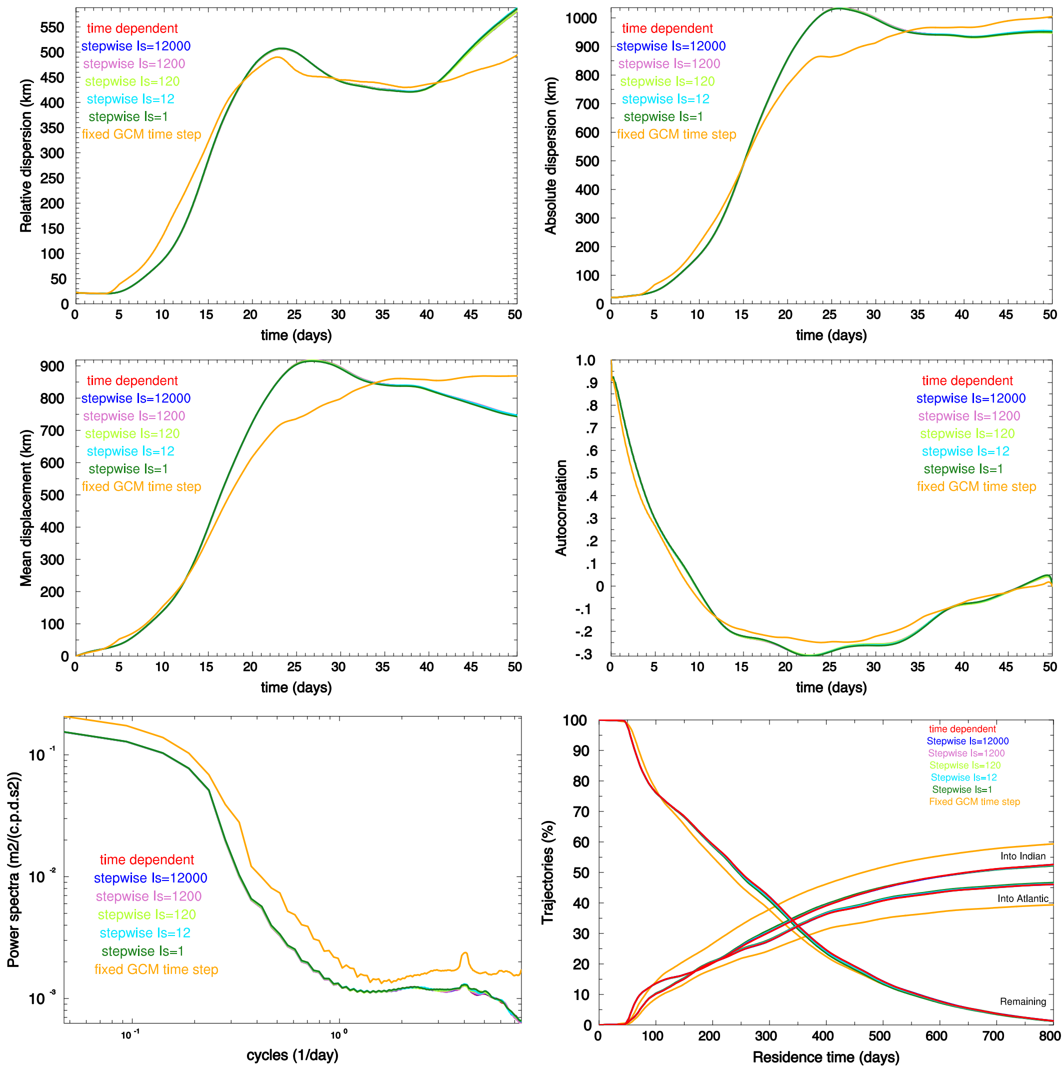

Figure 8. Lagrangian statistics of the ocean Agulhas trajectories. The relative dispersion (top left), the absolute dispersion (top right), the mean displacement travelled by the trajectory cluster (middle left), the average Lagrangian velocity autocorrelation of the trajectories (middle right). The average power spectra of the Lagrangian velocities (lower left). The residence time evolution of the trajectory particles in the Agulhas region. Note that all statistics show very similar results, where only those based on the "fixed GCM time step" (orange curves) differ from the rest.

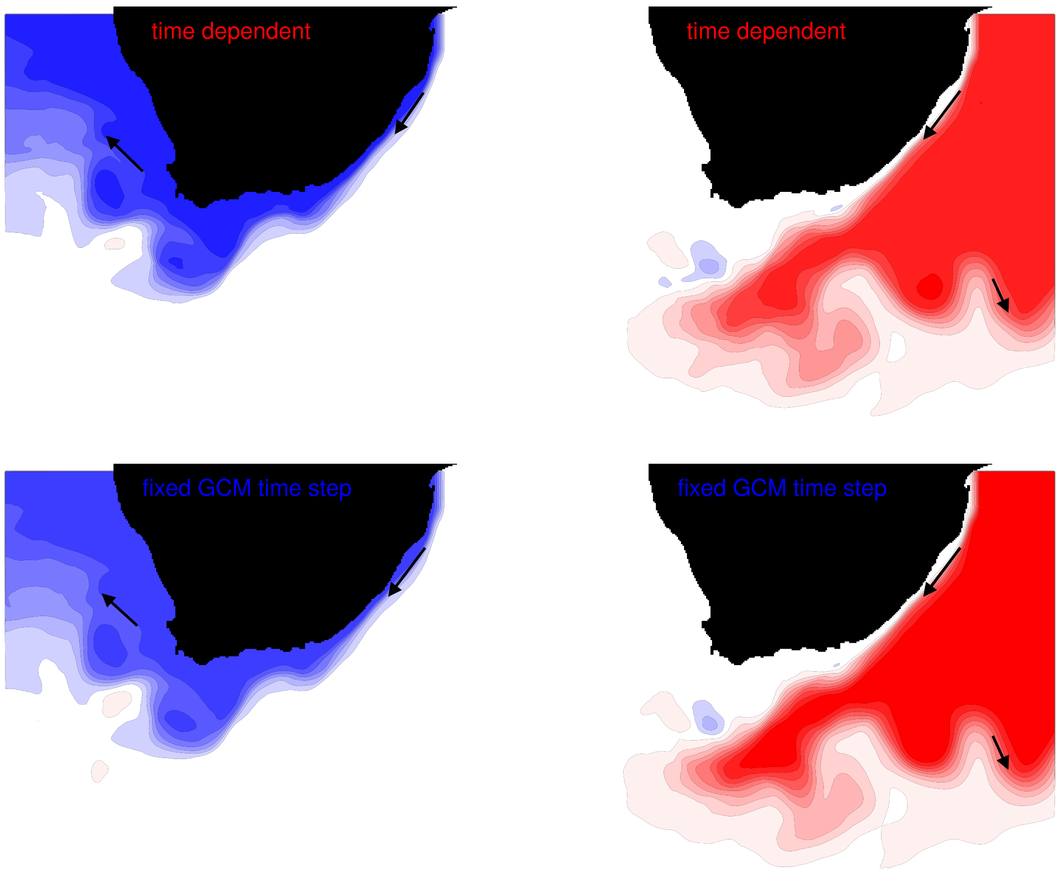

Figure 9. The Lagrangian decomposed barotropic stream function based on the particles released as previously but followed until they leave the Agulhas region into the Atlantic (left panels) or the Indan Ocean (right panels). The top panels with the "time-dependent" scheme and the lower panels with the "fixed GCM time step" scheme. Note that there is more water (one stream line extra) flowing into the Atlantic with the "time-dependent" scheme than with the "fixed GCM time steps" scheme, which instead favours relatively the flow into the Indian Ocean. Stream line intervals of 8 Sv $(10^6\, m^3/s)$.